

The Use of Volumetric Radar Reflectivity Predictors in the Development of a Second-Generation Severe Weather Potential Algorithm

JAY P. BREIDENBACH*

Research and Data Systems Corporation, Greenbelt, Maryland

DAVID H. KITZMILLER, WAYNE E. MCGOVERN, AND ROBERT E. SAFFLE†

Techniques Development Laboratory, Office of Systems Development, National Weather Service, Silver Spring, Maryland

(Manuscript received 3 August 1993, in final form 6 December 1994)

ABSTRACT

The operational WSR-88D Severe Weather Potential (SWP) algorithm is an automated nowcasting procedure aimed at providing guidance in the detection of severe local storms. It yields a numerical index proportional to the probability that an individual storm cell is producing, or will shortly produce, large hail, damaging surface winds, or tornadoes.

Currently, the SWP algorithm consists of a statistically derived function of the cell's maximum vertically integrated liquid and horizontal areal extent. In an attempt to refine the algorithm, a wide variety of new statistical predictors of severe weather have been derived from volumetric reflectivity observations. Experimental second-generation SWP equations incorporating these new predictors were evaluated and their skill was compared to that of the operational SWP algorithm.

Those predictors that parameterize the magnitude of the reflectivity in the middle and upper portions of convective storms were found to have the most diagnostic information with respect to severe weather. Some of these predictors rely only on reflectivity above 15 000 ft (4572 m) and thus could be applied to storms beyond the current algorithm's range of 230 km. The skill of the second-generation equations within 230 km was found to be comparable to that of the current algorithm.

1. Introduction

The intensity of thunderstorms has been estimated by the strength of weather radar reflectivity values for almost as long as radar observations have been available. Typically, operational radar observation has been limited to a single-base elevation angle unless a manual examination of higher levels was undertaken. One of the advantages of the Weather Surveillance Radar 1988 Doppler (WSR-88D) equipment being obtained through the triagency Next Generation Weather Radar (NEXRAD) program is its automatic volumetric scanning capability. A volume scan with information about the three-dimensional structure of storm reflectivity is built by "stacking" sweeps at various elevation angles on top of each other. From this process, many

new variables can be calculated that parameterize the reflectivity structure and intensity of thunderstorms.

The computation of the vertically integrated liquid (VIL) content of a thunderstorm was one of the earliest efforts to study the importance of volumetric reflectivity in severe storm and hydrological applications (Greene and Clark 1972). Objective use of VIL for severe weather specification was pioneered by Elvander (1977). The current WSR-88D SWP algorithm is based on this early work and considers several measures of VIL in producing its diagnostic-forecast output (Kitzmillier et al. 1992, 1995). The WSR-88D SWP is a generalized algorithm and is referred to as the severe weather *potential* rather than probability since the developmental data sample consists of observations from several radar sites, while the algorithm is applied at individual sites. Under these circumstances, the SWP is not intended to represent an absolute probability for individual sites, but rather an index that can be correlated to severe weather at all sites.

Here our goal is to thoroughly investigate the relationship of severe weather occurrence to a much larger set of variables derived from radar volumetric reflectivity data than were used in the initial SWP algorithm development. The purpose of this effort is to improve the accuracy and/or extend the range of the present

* Current affiliation: Hydrologic Research Laboratory, Office of Hydrology, National Weather Service, Silver Spring, Maryland.

† Current affiliation: Advanced Development and Demonstration Laboratory, Office of Systems Development, National Weather Service, Silver Spring, Maryland.

Corresponding author address: Jay P. Breidenbach, Office of Hydrology, NOAA/National Weather Service, W/OH3/jpb Rm #8370, 1325 East West Highway, Silver Spring, MD 20910.

WSR-88D SWP algorithm through the development of new second-generation SWP equations based on linear regression analysis.

2. Radar data

The radar data used in the development and testing of the new SWP predictors and algorithms were collected between 1985 and 1990 at WSR-57 and WSR-74 sites specially equipped with Radar Data Processor II (RADAP II) minicomputers. Those sites used in this study were Amarillo, Texas (AMA); Wichita, Kansas (ICT); Oklahoma City, Oklahoma (OKC); Binghamton, New York (BGM); and Tampa, Florida (TBW). The RADAP II system controls the radar for volumetric scanning and automatically archives reflectivity measurements. New volumetric scans were generally available every 10 or 12 minutes. Each datum in the archive represents reflectivity within a volume 2° in azimuth and 1 n mi (1.9 km) deep, at 2° increments in vertical resolution (McDonald and Saffle 1989). RADAP II data were also used in the development and testing of the first-generation WSR-88D algorithm. The RADAP II data include no velocity information and are coarser in resolution than that available from the WSR-88D. However, they were used exclusively in the development because of their availability over several geographic regions of the United States and their long period of record.

3. Objectively defined thunderstorm cells

All severe weather predictors were calculated from radar data objectively interpolated to 4×4 km elements of a horizontal grid extending to a radius of 230 km from the radar. At this resolution, a 2° beam is approximately 4 km wide at a range of 115 km, which is one-half the distance to the maximum range considered in this study. The interpolation scheme and grid size used here was chosen to match that used in the WSR-88D version of the VIL algorithm as defined in the NEXRAD Algorithm Report (1985). Since this interpolation scheme simply assigns the largest reflectivity value of all radar range bins located within the 4-km grid box, there could be a slight overestimation of some radar-derived variables. It also should be noted that at any given range the WSR-88D reflectivity bin size has nearly four times the resolution of the WSR-57 bin size and could cause the interpolation scheme to impart some additional overestimation of the 4-km VIL gridbox reflectivity. However, the statistical relationships discussed later should easily account for this small bias.

An individual storm "cell" was defined as a square region 28 km on a side (7×7 grid elements) centered on a local maximum in the VIL field. This size closely approximates the upper limit of the average spatial scale for individual thunderstorm cells as defined by Byers

and Braham (1949) to be between 10 and 30 km. In general, only cells having at least two grid elements with VIL of 10 kg m^{-2} or more were considered; the threat of severe weather is very small for cells less intense than this (Kitzmillier et al. 1992, 1995).

4. Tracking and association with severe weather reports

Each storm cell was tracked through its lifetime from one volume scan to the next and identified as severe or nonsevere according to the National Severe Storms Forecast Center log. By definition, a severe thunderstorm produces a tornado, wind gusts greater than or equal to 50 kt (25 m s^{-1}), and/or hail greater than or equal to 0.75 in. (1.9 cm) (Galloway 1989). Only cells traversing populated areas within 230 km of each radar site were included in the final statistical analysis since severe weather reports for such areas should best represent the actual fraction of cells with severe weather. This procedure yielded over 7000 storm cells at the five sites considered. The percentage of severe weather for the entire dataset was nearly 14%. The number of cells and percent severe for each individual site are shown in Table 1.

To create the predictor-predictand dataset needed in our equation development, it was necessary to choose one point in each cell's life history to describe that cell. For cells not associated with a severe weather report, that point was selected when the thunderstorm reached its greatest overall radar development, as defined by the sum of its VIL elements (SUMVIL). Similarly, cells associated with severe reports were described according to their peak development between 20 min before and 10 min after they produced severe weather. For cells featuring multiple severe events, the overall peak radar development was considered.

5. Explanation of volumetric reflectivity variables

For each cell described above, 49 predictors of severe weather occurrence were calculated from the volumetric reflectivity and entered into a database along with information on whether or not the storm was severe. The set of predictors included all of those used in the development of the first-generation SWP algorithm, as well as the new predictors discussed later in this section.

TABLE 1. Total number of thunderstorm cases, the number of severe, and the percentage of severe cases for each site.

Site	Cases	Severe	Percentage severe
BGM	355	122	34.4
AMA	1576	186	11.4
ICT	1627	231	14.2
OKC	2501	415	16.6
TBW	1064	49	4.6

Abbreviations and a short description of each of the predictors are shown in Table 2. Predictors 1 through 19 were originally defined by Elvander (1977, 1980) and studied using several years of data taken from the OKC radar. Jendrowski (1988) derived site specific equations using predictors 1 through 19 for both AMA and OKC found that many of these original 19 predictors were useful at both sites. These original 19 predictors all measure the magnitude and/or areal coverage of the VIL, which is directly related to the size and intensity of the thunderstorm. In general, larger cells are more likely to be severe. We have included these predictors again for further testing with a much larger dataset and with the new predictors. Those marked with a (1) are those used by the original first-generation SWP algorithm. Predictors 20 through 49, marked with a (2), are generally dependent on vertical reflectivity structure and were specifically derived for possible incorporation in a second-generation algorithm. They are referred to hereafter as "second generation."

We endeavored to develop new predictors that would be statistically related to severe weather and, at the same time, give some physical insight into the dynamics and structure of severe thunderstorms. For example, VIL potential energy (or VPE, in predictors 21, 22, 47, and 48) is an estimate of the geopotential of the precipitation mass in the storm. The VIL potential energy is largest when high concentrations of liquid water and hail exist at high altitudes in the cloud; such "precipitation loading" tends to increase the potential for downbursts (Roberts and Wilson 1989; Lee et al. 1992).

Area of overhang (OHANG, predictor 45) and volume of weak echo region (VOLWER, number 40) were calculated in the hope of distinguishing supercells. The overhang area was defined as the size of the area between 20 000 ft (6096 m) and 30 000 ft (9144 m) in which the 30-dBZ reflectivity existed above reflectivity of 18 dBZ or less below 10 000 ft (3048 m). The weak echo volume index was calculated in an attempt to identify the intense updrafts on the inflow side of supercells, which can cause a bounded region of low water content within the cell. Thus, VOLWER is defined as the volume of the region in which the reflectivity was less than 30 dBZ, while the surrounding reflectivity was at least 46 dBZ. This was an attempt to objectively parameterize the weak echo region as described by Lemon (1980).

Some of the second-generation predictors such as the maximum partial VIL above 15 000 ft (predictor 20) and the sum of the partial VIL above 15 000 ft (predictor 46) are similar to first-generation versions but focus more on the middle and upper portions of the storm. Predictors 32–35 indicate storm horizontal extent within various vertical layers. The volume occupied by reflectivity greater than various thresholds

(predictors 37–39) indicates the storm size and the size of its most intense core.

A large number of the predictors can be determined from the range–height indicator alone. The "vertically integrated VIP" (predictor 36) is an approximation to VIL; it is simply the sum of the VIP reflectivity levels observed over 10 000-ft deep layers to 50 000 ft. Predictors 23–31 are layer-maximum reflectivity values; 41–44 are maximum altitudes reached by various threshold reflectivities.

6. Individual predictor correlations with severe weather

Linear correlation coefficients were calculated between each predictor and severe weather occurrence at each site. The predictand was defined as 0 for nonsevere cells and 1 for severe ones. In Table 3, correlation coefficients are given for each predictor at BGM (representative of Northeast), AMA and ICT (Midwest), and TBW (Southeast). OKC was not used in Table 3 due to space considerations and because there is a significant overlap between the radar umbrellas of ICT and OKC. Due to this overlap we felt that the results from ICT should sufficiently represent this area of the country. Predictors have been listed in order from highest to lowest correlation to facilitate comparisons between individual predictors and comparisons between regions. Regional differences and the site specific nature of the first-generation SWP algorithm have been noted by Jendrowski (1988) and Kitzmiller et al. (1992).

A careful analysis of the important predictors from each region can reveal characteristics of severe storms that are common to that region. For example, at BGM, the three best predictors, N40VP3, VP00, and MXPV15, all depend on the areal extent or intensity of the mid- and upper-level reflectivity. If a storm contains a large amount of precipitation suspended aloft, a larger number of grid boxes with high reflectivity between 30 000 ft (9144 m) and 40 000 ft (12 192 m) will be observed. In addition, the potential energy of the precipitation and the VIL above 15 000 ft (4572 m) is likely to be greater in severe than in nonsevere storms. This result, showing the importance of mid- and upper-level reflectivity in the detection of severe thunderstorms, agrees with earlier findings by Donaldson (1965), Donaldson et al. (1975), and Lemon (1980), who have shown that updraft strength and subsequent precipitation loading as indicated by intense radar echoes aloft are important indicators of storm severity.

By comparing correlations and rankings of predictors at TBW with those from other sites, it is clear that storms in subtropical climates during the warm season (April through September) behave very differently from those found elsewhere. The percentage of cells with severe weather is very low, and none of the predictors exhibited a high linear correlation. The first

TABLE 2. Abbreviation and short description of volumetric radar reflectivity variables. Those marked with a (1) are used by the current SWP algorithm. Second-generation predictors are marked with a (2).

No.	Abbreviation	Description
1.	NSIZE	Number of grid boxes with $VIL \geq 10 \text{ kg m}^{-1}$
2.	MAXVIL	Max VIL value found anywhere in cell (kg m^{-2})
3.	VILWGT	(NSIZE)(MAXVIL)
4.	SUMVIL	Sum of the VIL values of cell grid boxes with $VIL > 10 \text{ kg m}^{-2}$
5.	AVGVIL	Average VIL = $SUMVIL/NSIZE$
6.	VIL-MASS	($SUMVIL$)($NSIZE$)
7.	VILMAS-FACT	VIL mass factor = $\sum i(NSIZE)$: Where NSIZE is number of grid boxes with $(i-1) 5 < VIL \leq i 5 \text{ kg m}^{-2}$
8.	MAXAVG	($MAXVIL$)($AVGVIL$)
9.	SVG10	1 Number of cell grid boxes with $VIL > 10 \text{ kg m}^{-2}$
10.	SVG15	Number of cell grid boxes with $VIL > 15 \text{ kg m}^{-2}$
11.	SVG20	1 Number of cell grid boxes with $VIL > 20 \text{ kg m}^{-2}$
12.	SVG25	Number of cell grid boxes with $VIL > 25 \text{ kg m}^{-2}$
13.	SVG30	Number of cell grid boxes with $VIL > 30 \text{ kg m}^{-2}$
14.	VMFG10	VIL mass factor using only $VIL > 10 \text{ kg m}^{-2}$
15.	VMFG15	VIL mass factor using only $VIL > 15 \text{ kg m}^{-2}$
16.	VMFG20	VIL mass factor using only $VIL > 20 \text{ kg m}^{-2}$
17.	VMFG25	VIL mass factor using only $VIL > 25 \text{ kg m}^{-2}$
18.	VMFG30	VIL mass factor using only $VIL > 30 \text{ kg m}^{-2}$
19.	VILEXS	$MAXVIL$ -average VIL (kg m^{-2})
20.	MXPV15	2 Max partial VIL above 15 000 ft (kg m^{-2})
21.	VPEM00	2 Max VIL potential energy (J m^{-2})
22.	VPEM15	2 Max VIL potential energy above 15 000 ft (J m^{-2})
23.	MAXR00	2 Max base-level reflectivity
24.	MAXR10	2 Max reflectivity between surface and 10 000 ft
25.	MAXR20	2 Max reflectivity between 10 000 and 20 000 ft
26.	MAXR30	2 Max reflectivity between 20 000 and 30 000 ft
27.	MAXR40	2 Max reflectivity between 30 000 and 40 000 ft
28.	MAXR50	2 Max reflectivity between 40 000 and 50 000 ft
29.	MAXR24	2 Max reflectivity between surface and 24 000 ft
30.	MAXR33	2 Max reflectivity between 24 000 and 33 000 ft
31.	MACR60	2 Max reflectivity between 33 000 and 66 000 ft
32.	N40VP3	2 Number of grid boxes greater than 40 dBZ (VIP 3) in 30 000-40 000-ft layer
33.	N40VP5	2 Number of grid boxes greater than 50 dBZ (VIP 3) in 30 000-40 000-ft layer
34.	N50VP3	2 Number of grid boxes greater than 40 dBZ (VIP 3) in 40 000-50 000-ft layer
35.	N50VP5	2 Number of grid boxes greater than 50 dBZ (VIP 3) in 40 000-50 000-ft layer
36.	VIVIP-MAX	2 Vertically integrated VIP (MAXIMUM)
37.	VOLGT3	2 Volume of storm with reflectivity greater than 40 dBZ (m^3)
38.	VOLGT5	2 Volume of storm with reflectivity greater than 50 dBZ (m^3)
39.	VOLTOT	2 Total volume of reflectivity greater than 18 dBZ (m^3)
40.	VOLWER	2 Volume of weak echo region (m^3)
41.	HGTVP3	2 Max height of the 40 dBZ (VIP3) reflectivity
42.	HGTVP5	2 Max height of the 50 dBZ (VIP5) reflectivity
43.	MAXTOP	2 Max height of the 18 dBZ (VIP1) reflectivity, i.e., max top
44.	HGTMAXR	2 Height of the max reflectivity
45.	OHANG	2 Area of overhang (m^2)
46.	SPVIL15	2 Sum of the partial VIL above 15 000 ft (kg m^2)
47.	SUMPE	2 Sum of the potential energy (J m^2)
48.	SUMPE-15	2 Sum of the potential energy found above 15 000 ft (J m^2)
49.	VRAIN	2 Vertical rainwater concentration = $Max VIL/MAXTOP$ (kg m^3)

generation predictors had linear correlations ranging from only 0.07 to 0.10. The best predictors appear to be those that indicate strong reflectivity extending to very high altitudes. For example, HVIP3, the height to which reflectivity of at least 40 dBZ extends, had the highest correlation coefficient, 0.17. The partial VIL above 15 000 ft (4572 m) and the VIL potential energy above 15 000 ft (4572 m) also had relatively high information content. Though VIL appears to yield relatively little information on storm severity in warm-season subtropical environments, it should be noted

that the Florida thunderstorm environment during the winter and early spring months more closely resembles that of the Plains than the typical warm season subtropical environment (Hagemeyer and Schmocker 1991). Thus, reflectivity-based severe weather detection techniques are probably most useful during the cool season for TBW. However, the RADAP II dataset did not have enough cool season cases to evaluate seasonal differences in algorithm performance in Florida.

The supercell detection predictors, OHANG and VOLWER, had low correlations with severe weather

TABLE 3. Linear correlation coefficients associated with each predictor listed in descending order for AMA, ICT, BGM, and TBW.

AMA			ICT		BGM		TBW			
Predictor		CC	Predictor	CC	Predictor	CC	Predictor		CC	
VILWGT	1	0.49	MAXAVG	0.52	N40VP3	2	HGTVP3	2	0.17	
VMFG30		0.48	N40VP3	2	0.52	VPPEM00	2	VIVIP-MAX	2	0.16
SUMVIL		0.48	MXPV15	2	0.51	MXPV15	2	H50VP3	2	0.15
VMFG10		0.48	SPVIL15	2	0.51	MAXVIL		MXPV15	2	0.14
SPVIL15	2	0.48	VILWGT	1	0.51	VILEXS		MAXR50	2	0.13
VILMAS-FACT		0.48	MAXVIL		0.49	SPVIL15	2	VPPEM15	2	0.13
VMFG15		0.48	VMFG25		0.49	VIVIP-MAX	2	MAXR40	2	0.13
VMFG25		0.48	SUMVIL		0.49	HGTVP3	2	VPPEM00	2	0.13
VMFG20		0.47	VMFG15		0.49	VILWGT	1	HGTMAXR	2	0.13
SVG30		0.47	VMFG20		0.49	MAX-TOP		SPVIL15	2	0.13
MAXAVG		0.47	VMFG30		0.49	MAXAVG		MAXVIL		0.13
MXPV15	2	0.46	VMFG10		0.48	SVG15		MAXR60	2	0.13
SVG25		0.46	VILMAS-FACT		0.48	VMFG10		SVG30		0.12
VOLGT5	2	0.45	N40VP5	2	0.47	VILMAS-FACT		MAXR33	2	0.12
MAXVIL		0.45	VOLGT5	2	0.47	SUMVIL		VMFG30		0.12
VOLGT3	2	0.44	SVG30		0.47	VMFG15		VILEXS		0.12
SVG15		0.44	VILEXS		0.46	SVG20	1	N40VP3	2	0.12
SVG20	1	0.44	SVG25		0.46	SVG10	1	MAXAVG		0.11
N40VP3	2	0.43	AVGVIL		0.46	SVG25		HGTVP5	2	0.11
VIL-MASS		0.43	VOLGT3	2	0.46	MAXR30	2	VMFG25		0.11
SVG10	1	0.43	HGTVP5	2	0.46	VMFG20		VILWGT	1	0.10
NSIZE		0.42	VIL-MASS		0.45	AVGVIL		AVGVIL		0.10
VILEXS		0.42	SVG20	1	0.44	NSIZE		SVG25		0.10
AVGVIL		0.41	N50VP3	2	0.44	VOLGT3	2	SUMVIL		0.10
N40VP5	2	0.40	SVG15		0.43	VMFG25		VILMAS-FACT		0.09
VIVIP-MAX	2	0.40	VIVIP-MAX	2	0.43	HGTVP3	2	VMFG20		0.09
HGTVP3	2	0.39	HGTVP3	2	0.42	SVG30		N40VP5	2	0.09
HGTVP5	2	0.38	HGTMAXR	2	0.41	VPPEM15	2	VMFG10		0.09
N50VP3	2	0.38	SVG10	1	0.40	VMFG30		VOLGT3	2	0.09
HGTMAXR	2	0.35	NSIZE		0.39	VOLGT5	2	MAXR30	2	0.09
SUMPE-15	2	0.34	N50VP5	2	0.39	SUMPE-15	2	VMFG15		0.09
MAXR50	2	0.33	VOLTOT	2	0.36	N50VP3	2	VIL-MASS		0.09
VOLTOT	2	0.32	MAXR50	2	0.36	MAXR00	2	VOLTOT	2	0.08
MAXR33	2	0.30	MAXR60	2	0.35	MAXR24	2	SUMPE-15	2	0.08
N50VP5	2	0.30	MAXR40	2	0.34	MAXR20	2	NSIZE		0.07
MAXR60	2	0.30	MAXTOP	2	0.33	VIL-MASS		SVG20	1	0.07
MAXR40	2	0.29	SUMPE-15	2	0.30	VOLTOT	2	VOLGT5	2	0.07
VPPEM00	2	0.28	MAXR33	2	0.29	SUMPE	2	SVG10	1	0.07
SUMPE	2	0.27	VPPEM15	2	0.27	MAXR60	2	SVG15		0.06
MAXR30	2	0.27	VPPEM00	2	0.27	MAXR10	2	MAXTOP	2	0.06
VPPEM15	2	0.25	VRAIN	2	0.27	MAXR50	2	OHANG	2	0.05
VRAIN	2	0.25	MAXR30	2	0.26	N40VP5	2	N50VP5	2	0.05
MAXR00	2	0.24	MAXR00	2	0.25	MAXR33	2	SUMPE	2	0.04
MAXR20	2	0.17	SUMPE	2	0.23	MAXR40	2	MAXR24	2	0.03
MAXR10	2	0.15	VOLWER	2	0.18	VRAIN	2	MAXR20	2	0.02
MAXR24	2	0.14	MAXR20	2	0.17	N50VP5	2	MAXR10	2	0.02
OHANG	2	0.14	MAXR24	2	0.16	HGTMAXR	2	MAXR00	2	0.02
MAXTOP	2	0.13	MAXR10	2	0.15	VOLWER	2	VOLWER	2	0.02
VOLWER	2	0.07	OHANG	2	0.15	OHANG	2	VRAIN	2	0.00

at all sites. Storms that feature a weak echo region or a significant overhang normally have a greater severe weather potential. However, it is likely that the vast majority of the storms in this study were not of the supercell type. Most severe storms in this database were probably strong multicells and squall lines, so that simple identification of supercells would not ensure effective detection of a broad spectrum of severe events. Also, the WSR-57 and WSR-74 systems, operating with a 2° beam, may not be able to adequately resolve these

features except at fairly close range. The WSR-88D should be able to detect these types of features more reliably, given its smaller 0.95° beamwidth. Finally, our use of a rather coarse 4 × 4 km horizontal reflectivity analysis could further complicate identification of some three-dimensional storm features.

Perhaps one of the most encouraging findings was that there are several predictors that may allow the range of the SWP algorithm to be increased. Total VIL cannot be reliably estimated beyond approximately 230

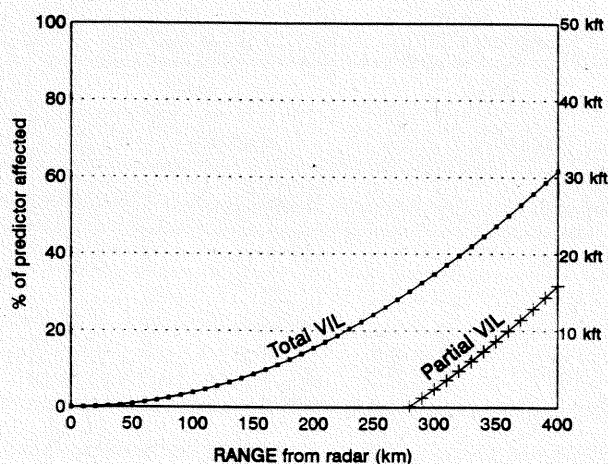


FIG. 1. The percentage of vertical depth eliminated in the calculation of Total VIL and Partial VIL for a 50 000-ft storm because it cannot be completely scanned due the earth's curvature. The right-hand legend shows the height of the lowest elevation radar beam in thousands of feet above ground level (total VIL) and above the 15 000-ft level (partial VIL).

km, given the effects of earth curvature and beam "overshoot" of the lower atmosphere. The current WSR-88D VIL algorithm deals with this problem by extrapolating the reflectivity value taken from the lowest elevation slice over the depth starting from the midpoint of the lowest two elevation slices down to the surface of the earth. This can lead to a significant under- or overestimation of the true VIL value depending on the actual vertical reflectivity distribution. While other factors such as attenuation, beam spreading, partial beam filling, and incomplete sampling of the reflectivity profile (Mahoney and Schaar, 1993) contribute to inaccuracies at long ranges, we believe beam overshoot is the biggest contribution to errors in the VIL calculation. To illustrate the range dependency of reflectivity variables derived from a given depth of a storm, consider the total VIL value and the partial VIL (above 15 000 ft) computed for a 50 000 ft tall storm (Fig. 1). At a range of approximately 230 km from the radar, the lower 20% of the storm needed for the total VIL calculation cannot be scanned by the radar. At 350 km, only 50% of the depth needed to calculate total VIL can be scanned. In contrast, the partial VIL value computed from data above 15 000 ft is not affected at all out to almost 300 km. At a range of 350 km, 80% of the necessary depth for an accurate calculation of partial VIL can still be seen by the radar.

At each site, there were several highly ranked predictors that involved only mid- and upper-level reflectivity. The partial VIL above 15 000 ft, the sum of the VIL above 15 000 ft, and the VIL potential energy above 15 000 ft all had relatively high correlations. This is clearly illustrated by comparing the correlations for maximum VIL (MAXVIL) and maximum partial VIL above 15 000 ft (MXPV15). At all five sites studied,

the correlation of the partial VILs to severe weather occurrences slightly exceeded the correlation of the total VIL to severe weather (Table 4). Furthermore, histograms showing the percentage of cells with severe weather for given ranges of VIL and partial VIL are almost identical (Fig. 2). This finding suggests that at ranges less than 230 km, little information is lost with respect to severe weather occurrence by eliminating the lower levels from the calculation of VIL. We believe that this result can be extended to ranges beyond 230 km where the total VIL value is severely impacted by loss of data at lower levels.

7. A closer look at individual predictor relationships to severe storm frequency

In section 8, we discuss the development of the linear regression equations that form the basis of our new second-generation SWP algorithm. These equations relate severe weather occurrence to a number of volumetric reflectivity variables. Since many of the predictor variables are highly intercorrelated, a large number of regression equations can be developed, each with a slightly different set of predictors. Before discussing the new equations, it is useful to examine, in detail, the relationships between a few individual predictors and severe storm frequency. Figures 3–5 illustrate this kind of analysis for several second-generation predictors.

For example, at AMA, if the volume of reflectivity greater than or equal to 40 dBZ (VOLGT3) is less than 992 km³, there is less than a 2% chance the storm will be severe, but with volumes above 2608 km³, there is a 35% chance the storm will be severe (Fig. 3). Physically, this tells us that storms with a large volume of high reflectivity are more likely to be severe. Although this variable did not have the highest correlation coefficient and was not selected by the regression equation, it illustrates the type of forecasting skill that can be expected by using this predictor or a similar one alone.

At BGM, the maximum VIL potential energy (VP EM00) was among the most highly ranked predictors, with a linear correlation coefficient of 0.40. Approximately 32% of all thunderstorms in this umbrella were severe. Of those cells with VP EM00 less than 60 J m⁻², only 11% were severe (Fig. 4). However, 62% of the storms with VP EM00 between 63 J m⁻² and 69 J m⁻² were severe. The VP EM00 index was able to categorize two-thirds of the storms into distinct low-potential (10% severe) and high-potential (62%

TABLE 4. Correlation of VIL and partial VIL with severe weather occurrence at AMA, BGM, ICT, OKC, and TBW.

	AMA	BGM	ICT	OKC	TBW
VIL	0.45	0.39	0.49	0.52	0.13
PARTIAL VIL	0.46	0.40	0.51	0.55	0.14

% CELLS W/SEV WX

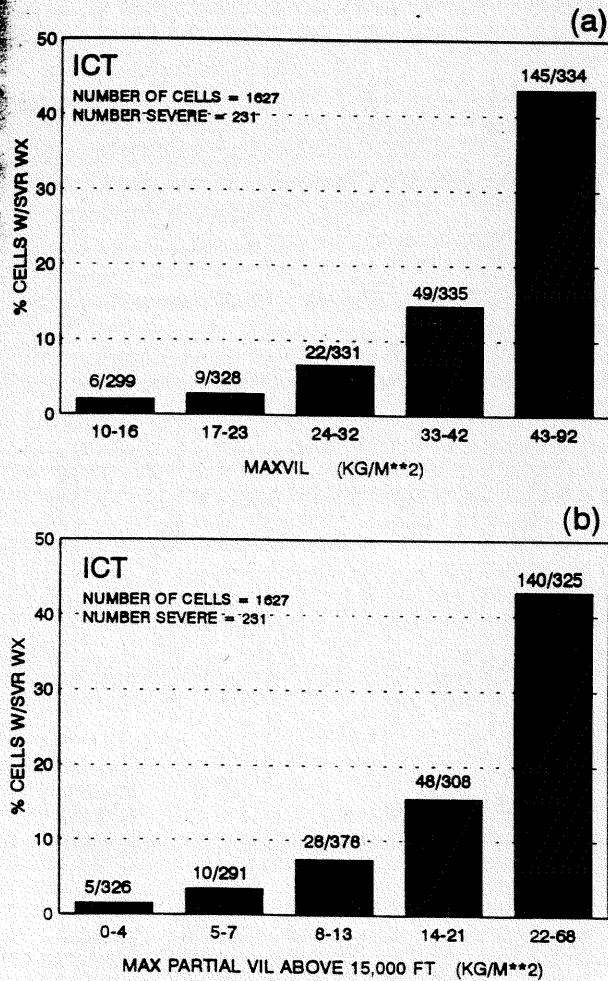


FIG. 2. Percentage of severe thunderstorm cells as a function of (a) the total VIL and (b) the partial VIL found above 15 000 ft at ICT.

severe) classes, which indicates a significant amount of diagnostic information.

At ICT, the most highly ranked predictor was N40VP3, the areal extent of the 40-dBZ (VIP 3) echo region in the 30 000–40 000-ft layer. As shown in Fig. 5a, over one-half of the storm cells (887 of 1627) did not feature 40-dBZ reflectivity in this layer, and only 3% of such cells were severe. For storms in which the 40-dBZ region covered 6–13 analysis grid boxes (approximately 100–200 km²), 27% were severe, while of those that had coverage of at least 14 boxes (224 km²), about 58% were severe (109/192).

At the same site, the predictor N50VP3, the areal extent of the 40-dBZ echo region in the 40 000–50 000-ft layer had a relatively low linear correlation (see Table 2). However, a further analysis of this index (Fig. 5b) showed that storms in which the 40-dBZ echo penetrates the 40 000-ft level have a significantly greater potential for severe weather than do shallower cells: 69

of 98, or 70%, for the deeper cells versus 10% (155 of 1520) for the shallower ones. Thus, the height of the 40-dBZ echo can be used to separate storms of rather low severe weather potential from those of high potential, for example, 3% if the height is under 30 000 ft (Fig. 5a) versus 70% if the height exceeds 40 000 ft (Fig. 5b). Of the few storms in which the areal echo coverage in this high layer exceeded 100 km² (category 6-25), over 90% were severe.

8. Development of the second-generation equations

Two types of second-generation equations relating severe weather occurrence to radar predictors were developed through forward-selection linear screening regression (see Draper and Smith 1985 for a complete description of forward-selection screening regression). The selection procedure was stopped when the added reduction of variance of the next predictor was less than 0.01. In addition, an *F* test was performed to confirm the significance of each equation. In the initial run, we allowed the screening regression to select from the full set of volumetric predictors (full). In the subsequent trial, we allowed only predictors that could be computed from radar data taken from the mid- and upper levels of storms (upper level). The upper-level equations, which do not include predictors below 15 000 ft, could be applied to storms beyond 230 km from the radar where doppler velocity and low-level reflectivity observations are not available. In addition, full and upper level equations were developed for each site (SITE SPECIFIC) and on data from a combination of sites (generalized) (see Table 5). The new equations and the operational WSR-88D first-generation SWP equation were then evaluated on independent data.

9. Evaluation of second-generation equations

When the new equations shown in Table 5 are examined, it is apparent that the screening regression

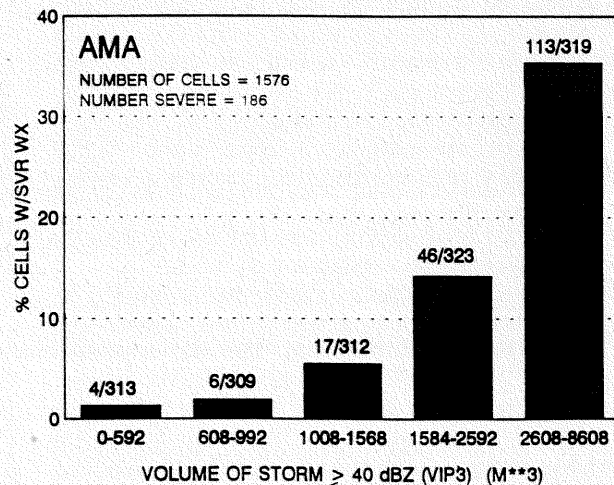


FIG. 3. Percentage of severe thunderstorm cells as a function of the volume of the storm greater than or equal to 40 dBZ at AMA.

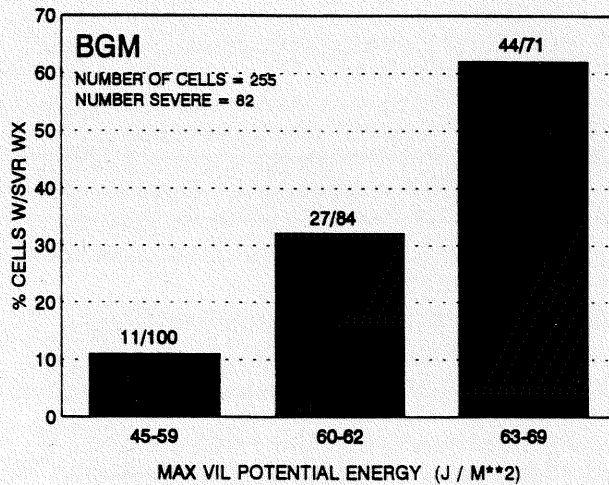


FIG. 4. Percentage of severe thunderstorm cells as a function of the maximum VIL potential energy at BGM.

consistently picked predictors that parameterize upper-level reflectivity even when the full set of predictors was available for selection. The sum of the partial VIL above 15 000 ft (SPVIL15), the maximum partial VIL above 15 000 ft (MXPV15), and the height of the VIP 5 (HGTVP5) were selected in several of the new equations. At BGM, the volume of the weak echo region (VOLWER) and the area of overhang (OHANG) were also selected as significant predictors in the regression equation. The percentage of variance explained by each equation is shown in Table 5. Notice that the new equations developed on data from a combination of sites explained more variance than the first-generation SWP equation. With the exception of TBW, site specific equations also explained more variance than the first-generation SWP equation. The ICT upper-level equation fit the dependent data best, reducing the variance by 34%.

It should be pointed out that the first-generation SWP equation and both equations from BGM contain predictors with a negative coefficient. Even though these predictors are positively correlated with severe weather when considered individually, it must be noted that the signs of the coefficients depend on the partial correlation to severe weather while the other selected predictors are held constant. Thus, it is not unusual for two intercorrelated predictors to have coefficients with opposite signs in a regression equation.

The various SWP equations were then evaluated on independent data from each site and on independent data from a combination of sites. The output of each equation is a probability or potential of severe weather occurrence for an individual cell. To assess the relative skill of the various equations, the probabilities were reduced to categorical (yes-no) forecasts by applying various thresholds. We verified each forecast by using NSSFC local severe storm reports. For each equation,

the Critical Success index (CSI) (Donaldson et al. 1975) was computed for the threshold needed to achieve a probability of detection (POD) of 0.7. The peak CSI (the highest CSI for any threshold regardless of the probability of detection) was also computed for each equation. It should be pointed out that CSI is not a completely unbiased estimate of warning skill (Schaefer 1990). However, CSI has been frequently used as a severe weather forecast evaluation tool by the National Weather Service. Here we use CSI mainly as means of comparing multiple-forecast equations for the same set of cases.

Before using the CSI to evaluate and compare our forecast equations, we determined that a variation in the CSI of less than 0.06 at a given site was probably not significant. This was determined by evaluating forecast equations at OKC on seven different independent datasets, each being taken from the same whole dataset. This experiment on the seven different inde-

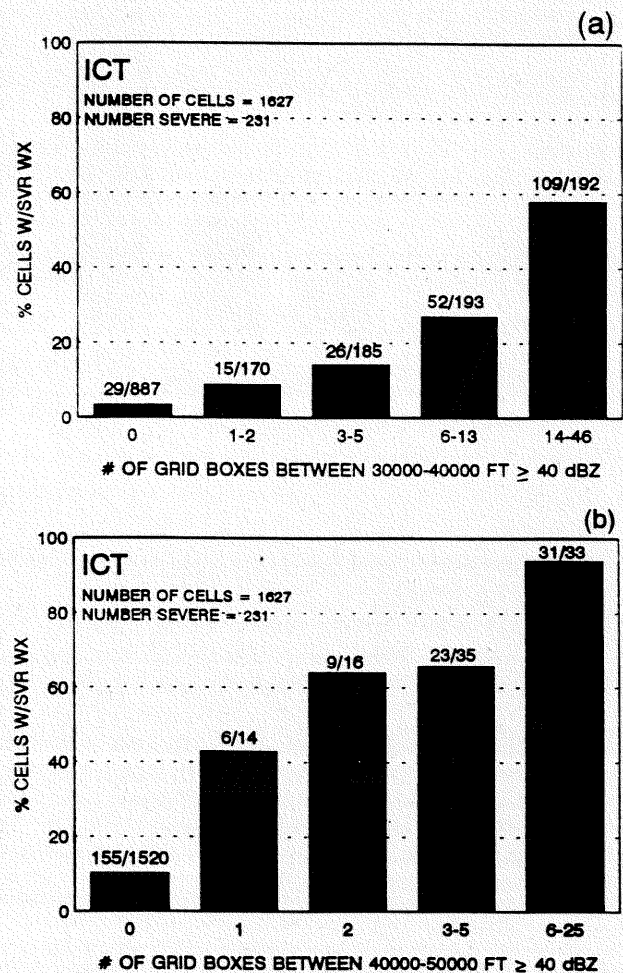


FIG. 5. Percentage of severe thunderstorm cells as a function of the number of 4×4 km grid boxes with reflectivity ≥ 40 dBZ (VIP3) at ICT between (a) 30 000 and 40 000 ft and between (b) 40 000 and 50 000 ft.

TABLE 5. SWP equations, their types, the number of cases used in the development, and the reduction of variance associated with each equation.

Type	SWP Regression equation	Cases	R Var%
WSR-88D SWP (first generation)	$5.850 + 0.046 (\text{VILWGT}) - 0.964 (\text{SVG10}) - 0.576 (\text{SVG20})$	4751	19.2%
Generalized (full)	$-2.187 + 1.172 (\text{VILEXS}) + 1.222 (\text{N40VP3})$	4751	24.2%
Generalized (upper level)	$-3.200 + 0.073 (\text{SPVIL15}) + 0.002 (\text{HGTVP5})$	4751	19.4%
Generalized excluding TBW (full)	$-3.401 + 0.935 (\text{MXPV15}) + 0.016 (\text{VILWGT})$	4041	26.4%
Generalized excluding OKC (full)	$-3.489 + 1.024 (\text{VILEXS}) + 0.046 (\text{SPVIL15})$	3038	21.5%
AMA (full)	$-1.683 + 0.030 (\text{VILWGT})$	1051	24.3%
AMA (upper level)	$-0.135 + 0.097 (\text{SPVIL15})$	1051	23.3%
BGM (full)	$4.544 + 3.630 (\text{N40VP3}) - 8.578 (\text{N40VP5}) + 0.738 (\text{MAXVIL})$ $+ 0.375 (\text{VOLWER}) + 0.729 (\text{OHANG})$	237	22.0%
BGM (upper level)	$11.963 + 3.283 (\text{N40VP3}) - 9.180 (\text{N40VP5}) + 1.330 (\text{MXPV15})$	237	19.0%
ICT (full)	$-3.132 + 0.016 (\text{MAXAVG}) + 1.354 (\text{N40VP3})$	1085	33.5%
ICT (upper level)	$-3.646 + 1.470 (\text{N40VP3}) + 0.002 (\text{HGTVP5}) + 0.988 (\text{N50VP5})$	1085	34.4%
OKC (full)	$2.479 + 1.354 (\text{MXPV15}) + 2.062 (\text{SVG30})$	1668	33.4%
OKC (upper level)	$-4.208 + 1.332 (\text{MXPV15}) + 0.060 (\text{SPVIL15})$	1668	32.8%
TBW (full)	$2.310 + 1.173 (\text{N50VP3})$	710	4.3%
TBW (upper level)	$2.310 + 1.173 (\text{N50VP3})$	710	4.3%

pendent datasets produced a range in peak CSI values of 0.09 and standard deviation of 0.03.

It is apparent from Table 6 that each type of equation had roughly the same CSI at an individual site. This means that generalized equations performed as well as a site-specific equation at any individual site. More importantly, there was little or no degradation in skill when only upper-level parameters were used in the predictive equation.

While there was not much variation in performance among the different types of equations at an individual site, there was significant variation in equation performance between sites. The equations performed best at BGM and OKC with peak CSI's greater than 0.40. Equations applied to TBW data had the poorest performance with CSI's in the 0.07-0.08 range. We speculate that the difference in skill observed between sites is likely caused by climatological differences in the storm environment and storm type, which lead to differences in the observed severe weather potential as defined by radar. A second reason for regional variation in skill could be caused by regional differences in severe storm verification efficiency. In our opinion, both factors played a large role in data collected at TBW. When

the TBW cases were excluded from the development sample for the generalized equation, we obtained a better fit to the data and explained a larger portion of the predictand variance.

10. Operational considerations

The values of CSI presented for the SWP equations here compare favorably with National Weather Service severe local storm warning verification statistics as reported by Grenier and Halmstad (1992). Nationally, there has been a continuous improvement in severe storm warnings over the decade of the 1980s as the national CSI has risen from 0.12 in 1980 to 0.38 in 1991. The national CSI is somewhat lower than the average CSI from the central, eastern, and southern regions, which have average CSI scores of 0.33, 0.43, and 0.48, respectively. The peak CSI scores (shown in Table 6) for the SWP algorithms discussed here indicate that it may be possible to implement automated algorithms that produce scores similar to those for non-automated warnings issued during the decade of the 1980s. However, it must be noted that CSI values computed for the SWP algorithm are based on a slightly

TABLE 6. Peak CSI for each equation at each site and the CSI for a POD of approximately 0.7 for each equation at each site.

Type of equation	Peak CSI for a given verification site						CSI for a POD - 0.7 at a given verification site					
	AMA	BGM	ICT	OKC	TBW	ALL	AMA	BGM	ICT	OKC	TBW	ALL
First-generation SWP	0.40	0.53	0.35	0.46	0.13	0.29	0.38	0.48	0.32	0.42	0.12	0.25
ALL (second generation)	0.36	0.56	0.39	0.53	0.12	0.32	0.36	0.39	0.29	0.50	0.11	0.27
ALL (upper level)	0.38	0.53	0.34	0.50	0.10	0.28	0.33	0.33	0.33	0.50	0.10	0.28
ALL (except TBW)	0.38	0.59	0.36	0.50	0.12	0.29	0.33	0.59	0.35	0.50	0.12	0.26
ALL (except OKC)	0.36	0.54	0.38	0.52	0.13	0.33	0.34	0.53	0.37	0.43	0.11	0.28
Site specific (second generation)	0.37	0.49	0.37	0.50	0.07	—	0.31	0.42	0.33	0.47	0.09	—
Site specific (upper level)	0.32	0.45	0.38	0.52	0.07	—	0.32	0.44	0.33	0.49	0.09	—

different verification criterion than that applied to local severe storm forecasts. The SWP scores may have a slight high bias when compared with those for local forecast offices. This is because the National Weather Service is required to verify its warnings for a specific locality such as a county, while our definition is based on a region near the path of an observed storm. Also, these SWP scores do not include severe events that are associated with very small storm cells (peak VIL less than 10 kg m^{-2}). Additional work by Polger et al. (1994) shows that scores at sites where the WSR-88D has been installed have drastically improved.

This suggests that SWP algorithms and future versions of the SWP can be used as an important guidance tool for the operational meteorologists making a warning decision similar to the way the Model Output Statistics (MOS) is used for making forecast decisions. In a severe weather situation, a forecaster should make use of all available products, especially base reflectivity and velocity products. The SWP value is probably most useful as an early warning-detection tool, especially in situations involving rapid storm development or multiple thunderstorms in the forecast area. Here, the SWP can point out storms that should be examined more thoroughly using all available products.

11. Conclusions and future work

We have shown that a wide variety of volumetric reflectivity variables can serve as predictors of severe weather occurrence. Some of the best new predictors are those that use reflectivity from the middle and upper layers of thunderstorms. The upper-level predictors are derived by sampling a layer whose lower bound does not change with increasing range; we may therefore expect to reduce range biases that may be observed with the total VIL and similar products. The second-generation equations that employ only upper-level predictors have nearly the same skill as those that use full volumetric data at ranges less than 230 km. Based on this result, it may be possible to assess storm severity at ranges well beyond 230 km to which the present WSR-88D SWP algorithm and doppler velocity coverage are now constrained. Recognizing the importance of upper-level reflectivity, it is suggested that an enhancement to the WSR-88D product suite could be made by computing and displaying the partial VIL above 15 000 ft. The partial VIL field would be immediately useful to forecasters, especially at longer ranges. In addition, a new generalized SWP equation, which uses the upper-level reflectivity field or partial VIL, could assess the severe weather potential at all ranges, in addition to providing new information beyond 230 km not currently available.

At ranges less than 230 km, the skill level of new second-generation equations was comparable to that of the first-generation SWP algorithm now in use by the WSR-88D. This may suggest that we are approach-

ing the limit of the predictive capability of reflectivity data alone. A third-generation SWP algorithm, which incorporates doppler velocity and spectrum width along with storm environmental parameters, will next be explored and is expected to provide considerable enhancement to forecasting skill, even at short ranges.

Acknowledgments. The development of the SWP algorithms discussed in this paper was made possible only because of the time and cooperation invested by National Weather Service field office personnel. They spent many hours archiving the raw radar data that were then forwarded to the Techniques Development Laboratory (TDL) for final processing. Without their support, such a large and unique RADAP II dataset could not have been collected.

We are also indebted to Melvina McDonald for her organization and monitoring of the RADAP II archive. We would also like to thank Paul Jendrowski, Michael Young, Thomas Renkevans, Jeffrey Peters, and Charles Gobs for the development of computer software used in the interpretation, editing, and statistical analysis of the radar data. Many of them also helped in the subjective severe storm identification process.

REFERENCES

- Byers, H. R., and R. R. Braham Jr., 1949: *The Thunderstorm*. U.S. Department of Commerce, Weather Bureau, 287 pp.
- Donaldson, R. J., Jr., 1965: Methods for identifying severe thunderstorms by radar: a guide and bibliography. *Bull. Amer. Meteor. Soc.*, **46**, 174-193.
- , R. M. Dyer, and J. J. Kraus, 1975: An objective evaluator of techniques for predicting severe weather events. Preprints, *Ninth Conf. on Severe Local Storms*, Norman, OK, Amer. Meteor. Soc., 321-326.
- Draper, N. R., and H. Smith, 1981: *Applied Regression Analysis*. John Wiley and Sons, 709 pp.
- Elvander, R. C., 1977: Relationships between radar parameters observed with objectively-defined echoes and reported severe weather events. Preprints, *10th Conf. on Severe Local Storms*, Omaha, NE, Amer. Meteor. Soc., 73-76.
- , 1980: Further studies on the relationships between parameters observed with objectively defined echoes and reported severe weather events. Preprints, *19th Conf. on Radar Meteorology*, Miami, FL, Amer. Meteor. Soc., 80-86.
- Galloway, J. G., 1989: The evolution of severe thunderstorm criteria within the National Weather Service. *Wea. Forecasting*, **4**, 585-592.
- Greene, D. R., and R. A. Clark, 1972: Vertically integrated liquid—a new analysis tool. *Mon. Wea. Rev.*, **100**, 548-552.
- Grenier, L. A., and J. T. Halmstad, 1992: Severe local storm warning verification: 1991. *NOAA Tech. Memo. NWS NSSFC-33*, National Oceanic and Atmospheric Administration, U.S. Department of Commerce, 20 pp. [NTIS PB92-1859982/AS.]
- Jendrowski, P. A., 1988: Regionalization of the NEXRAD severe weather probability algorithm. Preprints, *15th Conf. on Severe Local Storms*, Baltimore, MD, Amer. Meteor. Soc., 205-208.
- Kitzmilller, D. H., W. E. McGovern, and R. E. Saffie, 1992: The NEXRAD severe weather potential algorithm. *NOAA Tech. Memor. NWS TDL-81*, National Oceanic and Atmospheric Administration, U.S. Department of Commerce, 76 pp. [NTIS PB92197102.]
- , —, and —, 1995: The WSR-88D severe weather potential algorithm. *Wea. Forecasting*, **10**, 141-159.

- Lee, W. C., R. E. Carbone, and R. M. Wakimoto, 1992: The evolution and structure of a "bow-echo-microburst" event. Part I: The microburst. *Mon. Wea. Rev.*, **120**, 2188-2210.
- Lemon, L. R., 1980: Severe thunderstorm radar warning techniques and warning criteria. *NOAA Tech. Memor. NWS NSSFC-3*, National Oceanic and Atmospheric Administration, U.S. Department of Commerce, 60 pp. [NTIS PB 231409]
- Mahoney, E. A., and R. Schaar, 1993: WSR-88 Scan Strategy Impacts on the Vertically Integrated Liquid Product. Preprints, *26th Int. Conf. on Radar Meteorology*, Norman, OK, Amer. Meteor. Soc., 44-46.
- McDonald, M., and R. E. Saffle, 1989: RADAP II archive data user's guide. *TDL Office Note 89-2*, National Weather Service, NOAA, U.S. Department of Commerce, 16 pp. [Available from Techniques Development Laboratory, National Weather Service, 1325 East-West Highway, Silver Spring, MD, 20910].
- NEXRAD Algorithm Report, 1985: Vertically integrated liquid water algorithm description. NEXRAD Joint Systems Program Office, Washington DC, Chapter 6/24, 5-7.
- Polger, P. D., B. S. Goldsmith, R. C. Pryzwarty, and J. R. Bocchieri, 1994: National Weather Service Warning Performance Based on the WSR-88D. *Bull. Amer. Meteor. Soc.*, **75**, 203-214.
- Roberts, R. D., and J. W. Wilson, 1989: A proposed microburst nowcasting procedure using Doppler radar. *J. Appl. Meteor.*, **28**, 285-303.
- Schaefer, J. T., 1990: The critical success index as an indicator of warning skill. *Wea. Forecasting*, **5**, 570-575.

